

Rheological Evaluation of Kinetic Hydrate Inhibitors in NaCl/*n*-Heptane Solutions

Hassan Sharifi, Savvas G. Hatzikiriakos, and Peter Englezos

Dept. of Chemical and Biological Engineering, The University of British Columbia, Vancouver, BC, Canada V6T 1Z3

DOI 10.1002/aic.14433

Published online March 13, 2014 in Wiley Online Library (wileyonlinelibrary.com)

The performance of polyvinylpyrrolidone (PVP) and polyvinylcaprolactam (PVCap) as kinetic hydrate inhibitors (KHIs) in the presence of NaCl and n-heptane was evaluated by using a high-pressure cell in conjunction with a rotational rheometer. The addition of KHIs was found to prolong the induction time and decrease the hydrate growth. On the other hand, hydrates agglomerated more readily. PVP performed more efficiently than PVCap in delaying nucleation time but PVCap controlled the growth and delayed agglomeration more effectively. Addition of n-heptane to the system increased induction time and reduced growth. Unexpectedly, addition of KHIs in the presence of n-heptane decreased nucleation time but controlled growth effectively. Meanwhile, hydrate particles remained dispersed more efficiently and no agglomeration was detected. These observations confirm that high-pressure rheology is an additional laboratory assessment tool to evaluate KHIs under ocean field conditions. © 2014 American Institute of Chemical Engineers AIChE J, 60: 2654–2659, 2014

Keywords: gas hydrates, kinetic inhibition, flow assurance, liquid hydrocarbon, saline solution

Introduction

Oil and gas pipelines can be plugged by the formation of gas hydrates.^{1,2} Gas hydrates consist of small molecules trapped in the cavities formed by hydrogen-bonded water molecules. They are thermodynamically stable at high-pressure and low-temperature conditions.² Since the 1930s, prevention of gas hydrate formation has been accomplished by injection of thermodynamic inhibitors (mainly methanol and various glycols). It is estimated that more than \$200 million is spent annually to inhibit hydrate formation thermodynamically.³ Consumption of thermodynamic hydrate inhibitors will be higher for the applications in deeper water and more remote fields.^{4,5} Low-dosage hydrate inhibitors including kinetic hydrate inhibitors (KHIs) and antiagglomerates have been used as an alternative method to manage the risk of gas hydrate formation instead of prevention.⁵

KHIs are mostly water soluble polymers that prolong nucleation time and alter gas hydrate growth.^{5,6} The successful KHIs are polymers or copolymers containing vinyl-lactam monomers such as polyvinylpyrrolidone (PVP) and polyvinylcaprolactam (PVCap).⁷ KHIs are first tested in the laboratory and if they are successful, they are subsequently tested with field fluids and ultimately under field conditions.^{8–10} Although the adsorption–inhibition mechanism has been proposed to explain the KHIs' action,^{11,12} the mechanism of KHIs is not adequately understood yet. This lack of complete understanding does not allow the transferability of

lab-based results to industrial practice. In other words, it is not possible to predict how an additive may affect gas hydrate induction time and growth under field conditions.

If the contents of hydrocarbon multiphase pipelines are at thermodynamically favourable conditions (low temperatures and high pressures), hydrate crystal formation may occur.¹³ The solid hydrate particles may aggregate with time and can then block the flow.² Because gas hydrates are formed in pipelines, rheological properties would change and slurry viscosity increases.^{14–18} Hence, measurement of slurry viscosity either directly by using rheometers or by measuring pressure drops during hydrate formation can represent the growth and aggregation of hydrate crystals and particles. In other words, rheometry can be used as a sensor to detect the formation of and the extent of gas hydrate crystal growth and agglomeration.^{18,19} KHIs could alter the gas hydrate growth and consequently hydrate slurry viscosity. Therefore, the effect of kinetic inhibitors on gas hydrate nucleation and growth can be examined by using rheometry as a diagnostic tool to compare the changes in the viscosity of the hydrate suspension in the presence and absence of KHIs as a function of time.

The effect of KHIs on gas hydrate formation has been studied extensively under different conditions and by using various experimental approaches.^{20–28} In this work, a high-pressure cell in conjunction with a rotational rheometer is used to assess the performance of two commercial kinetic inhibitors under more realistic conditions including: multi-component gas mixture, high driving force, presence of sodium chloride, and liquid hydrocarbon (*n*-heptane). To the best of our knowledge, the following is the first study that evaluates the performance of kinetic inhibitors by direct

Correspondence concerning this article should be addressed to P. Englezos at peter.englezos@ubc.ca.

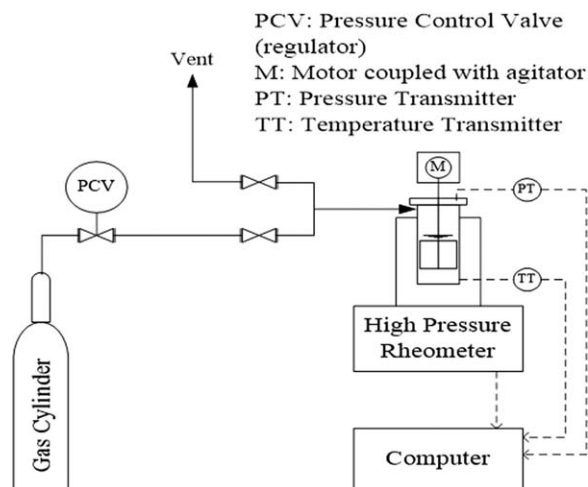


Figure 1. Schematic of the experimental setup.

measurement of viscosity changes of gas hydrate slurries formed *in situ* at high-pressure conditions.

Experimental Section

Materials

Saline solutions (3.5 wt %) were prepared by dissolving granulated NaCl (provided by Fisher Scientific) in deionised and distilled water. PVP (average molecular mass of 3.5 kDa; Acros Organics) and PVCap solution (40 wt % PVCap in ethanol; average molecular mass of ~ 23.3 kDa; BASF) were used to make 0.1 mM of kinetic inhibitor in 3.5 wt % NaCl aqueous solutions. A natural gas mixture (UHP grade) consisting of methane/ethane/propane with the mole ratio of 93/5/2 was supplied by Praxair Technology. The liquid hydrocarbon used in the experiments was *n*-heptane that was purchased from Fisher Scientific.

Apparatus

The Physica MCR 501 rheometer from Anton Paar equipped with a high-pressure cell²⁹ was used. Figure 1 shows the schematic of the experimental setup. The rheometer could control either stress or strain. It had a torque range from 0.1 $\mu\text{N m}$ to 150 mN m with the resolution of 0.1 nN m . The resulting uncertainty in the viscosity measurement is 0.5 $\mu\text{Pa s}$. The Rheoplus software was used to calibrate the instrument, setup and run the experiments, and analyze the raw experimental data. The pressure cell consisted of a stainless steel chamber (internal diameter of 27.11 mm and length of 75 mm) and a stainless steel vane (dia. 24.62 mm) with four blades (cup-and-bob) assembly. Thus, the geometry had a 1.24 mm gap between the tip of the blade and the chamber wall. The cell was designed to operate up to 15.0 MPa. The pressure was measured by a sealed gauge pressure transmitter PA-23 from Keller, with the maximum uncertainty of 40 kPa. The pressure cell fitted in a Peltier temperature control system and was mounted on the rheometer. The Peltier jacket had a temperature range from 243.15 to 473.15 K, with the maximum cooling and heating rate of 4 and 8 K/min, respectively. The temperature was measured by a thermocouple with the maximum uncertainty of 0.1 K. A water bath supplied the jacket with cooling fluid to sink heat. The temperature probe was embedded in the shell of the cell.

Hence, the solution temperature could be readily detected. Pressure, temperature, slurry viscosity, and applied torque were recorded during the experiments.

Gas hydrate formation

In hydrate-formation experiments, either 18 mL of the desired aqueous solution or 12 mL of aqueous solution plus 6 mL of *n*-heptane was loaded to the cell. PVP and PVCap are water-soluble polymers⁵ and are expected to remain in the aqueous phase in the presence of *n*-heptane. Therefore, the addition of *n*-heptane is not expected to dilute the KHI solutions. The solution temperature was adjusted to 293.15 K. Subsequently, the chamber was pressurized with the desired gas mixture up to a pressure less than that required for equilibrium hydrate formation and then depressurized three times to remove air from the system. Afterward, the cell was pressurized to 8.0 MPa with the desired gas mixture, and a shear rate of 100 s^{-1} was applied. The system pressure was monitored and kept constant at 8.0 MPa (through the gas cylinder regulator) for 10 h to saturate the liquid phase with the gas mixture. Finally, the system was isolated (batch protocol) and a temperature program was applied. This marked the starting point of the experiments. The temperature program included two steps (Figure 2): ramping and isothermal. In the first step, the cell was cooled down from 293.15 to 274.15 K at the rate of 20 K/h. At 293.15 K and 8.0 MPa the mixture is outside of the hydrate stable region because the equilibrium hydrate formation temperature for the desired gas mixture at 8.0 MPa is 289.3 K.³⁰ The temperature was kept constant at 274.15 K during the second step. Also, the shear rate was 100 s^{-1} . The temperature, pressure, torque, and viscosity were measured throughout the process of hydrate formation. Once the solution viscosity reached a value approximately equal to 4 Pa s, the hydrate formation experiment was terminated for the sake of safety. The number of moles of gas consumed to form gas hydrate at any given time was calculated as described.³¹

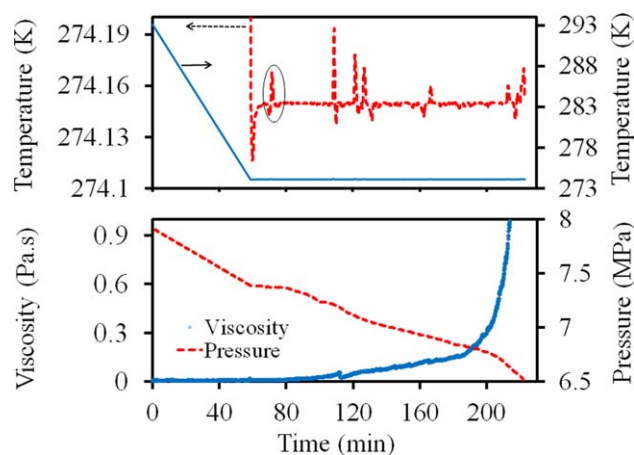


Figure 2. Pressure, temperature, and viscosity profiles during hydrate formation in saline solution (control).

In the top graph, solid blue line shows the temperature profile in both ramping and isothermal parts while dashed red line depicts the temperature profile in the isothermal section. The onset of hydrate formation is noted at about 71 min after the start of the experiment. [Color figure can be viewed in the online issue, which is available at wileyonlinelibrary.com.]

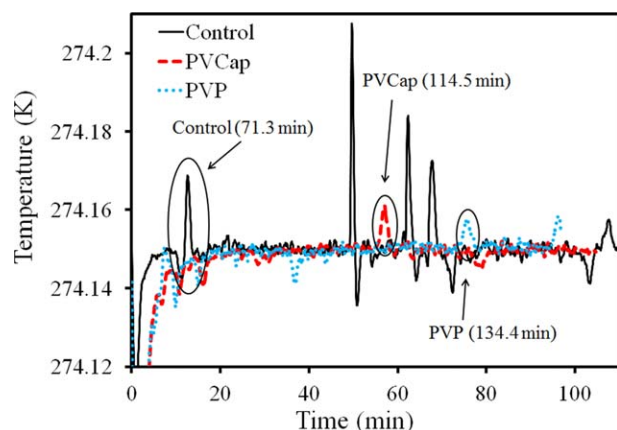


Figure 3. Temperature profiles during hydrate formation in saline solutions with and without inhibitors (PVP or PVCap).

The zero time corresponds to the start of the isothermal stage at 274.15 K. It took 57 min to cool down the system from 293.15 to 274.15 K at the rate of 20 K/h during the ramping stage. [Color figure can be viewed in the online issue, which is available at wileyonlinelibrary.com.]

Results and Discussion

Gas hydrate nucleation, growth, and agglomeration in the saline solutions

As gas hydrate formation is an exothermic process,² a spike in aqueous phase temperature along with a sudden reduction in gas-phase pressure would indicate the nucleation point of hydrate formation. An increase in the viscosity of the liquid phase along with a decrease in pressure would represent hydrate crystal growth. Figure 2 shows pressure and temperature profiles during hydrate formation in saline solution (control) and the viscosity profile of the hydrate slurry. As seen in the figure, during the temperature ramping step from 293.15 to 274.15 K the pressure is reduced by about 0.6 MPa due to temperature reduction. As there is no change in viscosity and no change in the slope of the pressure curve and no temperature spikes, it is concluded that there is no hydrate formation during the ramping step. The observed spikes in the temperature profile represent hydrate nucleation points. In subsequent figures, only the isothermal part of the profiles will be featured because hydrates did not form earlier.

Figure 3 shows temperature profiles during hydrate formation in saline solutions with and without inhibitors. As seen in this figure, temperature spikes are detected in both cases. The induction times are: 71.3 min for saline solution without inhibitor (control), 114.5 min for the solution with PVCap, and 134.4 min for the solution with PVP. The induction times along with other experimental information are seen in Table 1. As expected, addition of inhibitors increased hydrate nucleation time.⁵ In the presence of PVCap, the induction time increased almost 1.6 times compared to the time for saline solution with no inhibitor, and in the presence of PVP, the induction time increased almost two times. Here, PVP performed more effectively compared to PVCap in terms of prolonging the induction time. These results are in agreement with our previous work³² by using autoclave crystallizers and high-pressure microdifferential scanning calorimeter for evaluation of PVP and PVCap.

It is not completely clear how KHIs influence the hydrate inhibition. The adsorption–inhibition mechanism has been proposed^{12,33,34} for the performance of KHIs. It was shown that the ratio of dissipation factor which represents viscoelastic properties of adsorbed layer^{35,36} to the adsorbed mass might be a useful factor to evaluate the performance of kinetic inhibitors²⁷; in which, the lower the ratio value, the better the performance as KHIs. Zeng et al.²⁷ measured this ratio for PVP and PVCap and showed that more PVP molecules adsorbed on the surfaces with higher dissipation factor. Thus, the ratio of dissipation factor to the adsorbed mass was higher for PVP compared to PVCap. They measured the dissipation factor for high molecular weight PVP (~40 kDa). Low-molecular weight PVP was used in this work and this is expected to indicate a decreased dissipation factor.³⁵ Hence, the ratio of dissipation factor to the adsorbed mass for PVP molecules might be lower than when PVCap is used.

Continuous pressure reduction leads to hydrate growth after the crystal nucleation and this causes an increase in total consumed gas reflecting the gas hydrate growth in the NaCl (3.5 wt %) solution. Figure 4 illustrates the cumulative gas consumption and viscosity profiles for the saline solutions with and without inhibitor during hydrate formation in the isothermal step.

Based on data in Table 1 and Figure 4, the addition of PVP and PVCap to saline solutions controlled gas hydrate growth and reduced cumulative gas consumption. PVP decreased gas hydrate growth rate by about 72% compared

Table 1. Experimental Solutions and Results Showing Induction Times, Growth Rates, and Agglomeration Times

Gas Mixture: Methane (93%), Ethane (5%), Propane (2%)		Induction Time (min)		Growth Rate (mmol/min)		Sudden Rise in Viscosity (Agglomeration Time) (min)	
Experiment	Solution	Average		Average		Average	
1A	Control	72.1	71.3	0.195	0.198	143	146
1B		70.5		0.201		150	
2A		130.7	134.4	0.053	0.055	91	94
2B	PVCap	138.1		0.057		97	
3A		111.6	114.5	0.0163	0.017	96	99
3B		117.4		0.0177		102	
4A	Control + heptane	214.6	218.9	0.0123	0.0126	352	366
4B		223.2		0.013		370	
5A	PVP + heptane	123.2	124.9	0.00274	0.0027	Not observed	
5B		126.6		0.00267			
6A	PVCap + heptane	158.8	160.1	0.00183	0.0018	Not observed	
6B		161.4		0.00176			

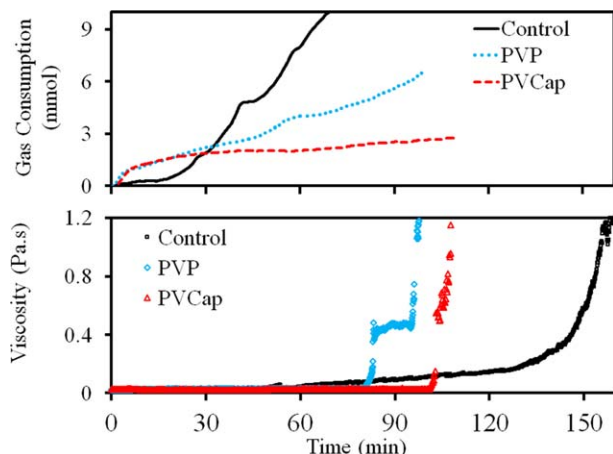


Figure 4. Cumulative gas consumption and hydrate slurry viscosity profiles during hydrate formation in saline solutions with and without inhibitors (PVP or PVCap) under isothermal condition ($T_{\text{exp}} = 274.15$ K, initial $P_{\text{exp}} = 8.0$ MPa).

Gas consumption data for saline solutions without inhibitors were collected up to 150 min but they are not shown to preserve the y axis scale. [Color figure can be viewed in the online issue, which is available at wileyonlinelibrary.com.]

to the case without inhibitor (from 0.198 to 0.055 mmol/min). However, in the presence of PVCap the growth rate decreased almost 92% (from 0.198 to 0.017 mmol/min). Although PVP performed better than PVCap in terms of increasing the induction time, PVCap reduced hydrate growth rate more effectively. The effectiveness of PVCap compared to PVP in controlling gas hydrate growth might be related to the multilayer adsorption of PVCap on hydrate crystals.³⁷ It is then possible that the thickness of the adsorption layer in the presence of PVCap is greater than that with PVP and this in turn may decrease the diffusion of hydrate formers from the bulk phase to the growing hydrate crystals surface. However, we have no evidence of the relative thickness of the adsorption layers.

Due to the formation and agglomeration of hydrate particles, hydrate slurry viscosity increased in saline solutions with or without inhibitors (Figure 4). Hydrate crystals begin forming after 20 min (nucleation time ~ 20 min; Figure 3) while no increase in solution viscosity was detected until about 60 min (Figure 4), which indicates that the formed hydrate particles were small enough that could not change the slurry viscosity effectively. Then, the saline solution viscosity rose gradually with an almost constant rate at 0.0016 Pa s/min up to 0.154 Pa s (at 126 min). This indicates the formation of more hydrate particles, which were still dispersed. Afterward, a sharp increase in viscosity was observed (at 146 min), which might be related to the agglomeration of hydrate particles and would be considered as analogous to pipeline blockage. Remarkably, addition of PVP and PVCap promoted hydrate particles agglomeration (Figure 4).

In the presence of PVP, the solution viscosity did not increase until 78 min indicating less hydrate crystals formed compared to the control case, which is shown in Figure 4. A first drastic increase in viscosity (from 0.0172 to 0.461 Pa s) was observed at 78 min and after 16 min (at 94 min) the second rise of viscosity was detected. At this point, the rhe-

ometer was stopped for the safety reasons. These increases in viscosity might be related to the agglomeration of hydrate particles. The agglomeration and accumulation of hydrate crystals is linked to the plugging of hydrocarbon transport pipelines. The addition of PVCap had similar effect on the viscosity (Figure 4). In this case, an increase in viscosity was not observed up to 99 min while, after that, the viscosity increased drastically which indicates hydrate agglomeration. Although addition of KHIs increased induction time and decreased consequent hydrate growth, it seems that these additives might increase hydrate particles adhesion tendency as evidenced by the viscosity of the suspension. Therefore, in the presence of PVP and PVCap, the gas hydrate slurry formed is not processable after 94 and 99 min, respectively, as opposed to the case without inhibitors (146 min). Thus, KHIs regulated growth up to a certain point after which a sharp increase in viscosity was detected probably due to hydrate particle agglomeration. Such occurrence in the field would be undesirable.

Gas hydrate nucleation, growth, and agglomeration in saline solutions and in the presence of a liquid hydrocarbon phase

Figure 5 shows the temperature profiles in the presence of *n*-heptane in saline solutions with and without inhibitors. The addition of *n*-heptane had a significant effect on gas hydrate nucleation. As seen in Figure 5, induction time increased to 218.9 min by addition of *n*-heptane to saline solution. In this case, induction time increased by almost a factor of three (Figures 3 and 5 and Table 1). Under the same pressure of 8.0 MPa, the addition of *n*-heptane reduces the hydrate equilibrium temperature^{38,39} from 289.7 to 286.5 K for the gas mixture used in this work (calculated by CSMGem³⁰). Therefore, less driving force ($T_{\text{eq}} - T_{\text{exp}}$) is provided in the presence of *n*-heptane. On the other hand, as gas molecules have to diffuse through the *n*-heptane layer to reach the aqueous saline solution and form hydrate, consequently,⁴⁰ the presence of *n*-heptane provides an extra mass-

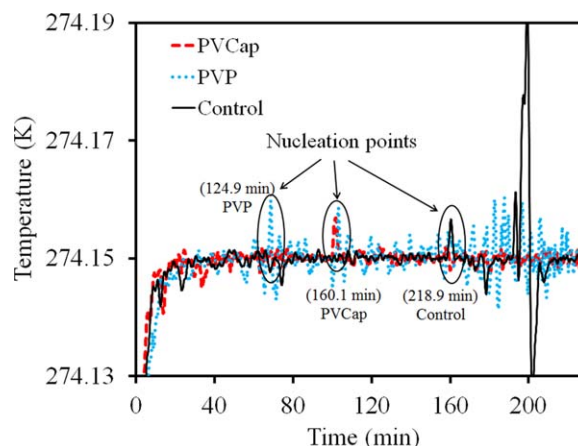


Figure 5. Temperature profiles during hydrate formation in the presence of *n*-heptane in saline solutions with and without inhibitors (PVP or PVCap) with a cooling rate of 20 K/h and initial pressure of 8.0 MPa.

The zero time corresponds to the start of the isothermal stage at 274.15 K. [Color figure can be viewed in the online issue, which is available at wileyonlinelibrary.com.]

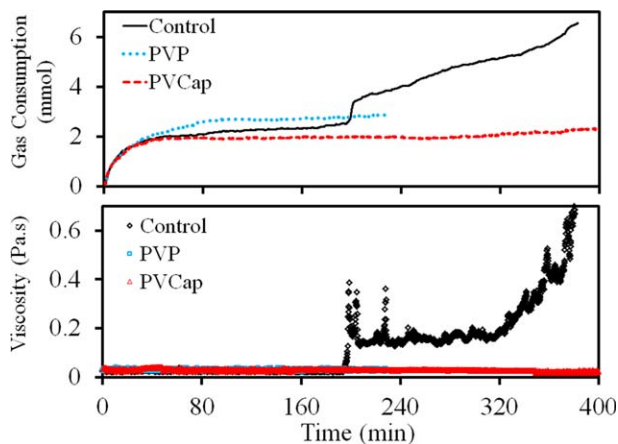


Figure 6. Cumulative gas consumption and hydrate slurry viscosity profiles during hydrate formation in saline solutions with and without inhibitors (PVP or PVCap) in the presence of heptane under isothermal condition ($T_{\text{exp}} = 274.15 \text{ K}$, initial $P_{\text{exp}} = 8.0 \text{ MPa}$).

[Color figure can be viewed in the online issue, which is available at wileyonlinelibrary.com.]

transfer resistance to the gas diffusion. These two factors might be the likely cause of increase in hydrate nucleation time by addition of *n*-heptane.

Figure 5 shows that by addition of PVP and PVCap to saline solutions in the presence of heptane, hydrate nucleation point decreased to 124.9 and 160.1 min, respectively. Therefore, in spite of the fact that addition of KHIs to an aqueous saline solution increases the induction time, the addition of the inhibitors to saline solution in the presence of *n*-heptane accelerates hydrate formation (decreases the induction time). The reason for this impact is not clear, but it might be related to the influence of PVP and PVCap on interfacial surface tension between aqueous solution and *n*-heptane phase. It was reported that addition of PVCap and PVP to the aqueous phase can decrease the interfacial tension between the organic and aqueous phases (from 50 to 20 mNm^{-1}).^{41,42} Thus, the contact between these two-phases would increase, which in turn can reduce the mass-transfer resistance against gas diffusion. In the presence of *n*-heptane, PVCap acted more effectively than PVP (Figure 5) in terms of increasing of induction time, which is in contrast with the case of without *n*-heptane. This observed behavior could have serious implications to field deployment of inhibitors if it is not taken into account.

Continued pressure reduction after the nucleation point indicates hydrate crystal formation. Figure 6 depicts the cumulative gas consumption and the hydrate slurry viscosity profile during hydrate formation with and without inhibitors in saline solution and in the presence of *n*-heptane. Based on the data shown in Figure 6, in the presence of *n*-heptane the gas hydrate growth rate is about 0.0126 mmol/min. This growth is less than the growth observed in saline solutions without *n*-heptane (0.198 mmol/min). This reduction in gas hydrate growth rate can be correlated with the decrease in driving force and the existence of extra mass-transfer resistance as discussed above.

Moreover, the presence of KHIs in saline solution and in the presence of *n*-heptane also reduced gas hydrate growth (Figure 6 and Table 1). In this case, the rate of gas hydrate growth in PVCap experiments (0.0018 mmol/min) was slower than that in PVP ones (0.0027 mmol/min). Perhaps,

the multilayer adsorption of PVCap molecules on hydrate crystal's surfaces might cause better performance of PVCap in reducing of hydrate growth rate.³⁷

As seen in Figure 6, the hydrate slurry viscosity started rising at the 196th minute, whereas in the absence of *n*-heptane this occurred at the 60th minute (Figure 4). In the presence of *n*-heptane, the sharp increase in the hydrate slurry viscosity corresponding to the hydrate agglomeration was prolonged to 366 min (Figure 6 and Table 1) compared to the case without *n*-heptane (146 min as seen in Figure 4 and Table 1). This means that the addition of the liquid hydrocarbon decreased hydrate particle tendency for agglomeration. This implies that in a pipeline and in the absence of inhibitors, there will be a delay in pipeline blockage simply by the presence of a liquid hydrocarbon phase.

Figure 6 also depicts the effect of *n*-heptane addition on the viscosity profile for gas hydrate slurries in the presence of PVP and PVCap. However, as seen in the figure, the slurry viscosity did not rise after a while compared to the case without inhibitor. This observation indicates that gas hydrate particles might remain dispersed. It is noted that a similar observation was made in a stirred vessel with the addition of PVCap in a 3.5 wt % NaCl solution and in the presence of liquid hydrocarbon.³⁹ These results show that although induction times decreased by the addition of KHIs in the presence of *n*-heptane, hydrate growth rate decreased drastically and hydrate agglomeration did not happen for long period of time studied in this work.

Conclusions

Direct viscosity measurement of hydrate slurries by using a high-pressure rheometer was used to evaluate the performance of two KHIs, namely PVCap and PVP, in the presence of NaCl and *n*-heptane. It was found that in the presence of inhibitors in saline solution, hydrate nucleation was delayed with PVP performing more effectively than PVCap. Both kinetic inhibitors controlled the gas hydrate growth immediately after nucleation but they increased hydrate particles tendency to agglomerate. PVCap controlled hydrate growth more effectively than PVP. The addition of liquid hydrocarbon (*n*-heptane) to saline solution delayed the onset of hydrate formation was accompanied by a reduction in the hydrate crystal growth and a delay in hydrate agglomeration. Unexpectedly, the addition of KHIs in saline solution in the presence of *n*-heptane accelerated hydrate nucleation. In addition, gas hydrate growth decreased significantly by the addition of KHIs to saline solution in the presence of *n*-heptane and hydrate particles remained dispersed in the slurry phase thus minimizing chances of pipeline blockage.

Acknowledgments

Authors thank Dr. J.D. Lee, KITECH, Korea, for providing PVCap for this work and Ehsan Behzadfar, PhD candidate at the University of British Columbia, for his guides in operating the high-pressure rheometer. The financial support from the Natural Sciences and Engineering Research Council of Canada (NSERC) is greatly appreciated.

Literature Cited

1. Ellison BT, Gallagher CT, Frostman LM, Lorimer SE. The physical chemistry of wax, hydrates, and asphaltene. In: *Offshore Technology Conference*. Houston, TX, OTC 11963, 2000.
2. Sloan ED, Koh CA. *Clathrate Hydrates of Natural Gases*. CRC Press LLC, Boca Raton, FL, 2008.

3. Sloan ED. Fundamental principles and applications of natural gas hydrates. *Nature*. 2003;426(6964):353–363.
4. Koh CA. Towards a fundamental understanding of natural gas hydrates. *Chem Soc Rev*. 2002;31(3):157–167.
5. Kelland MA. History of the development of low dosage hydrate inhibitors. *Energy Fuels*. 2006;20(3):825–847.
6. Sloan ED, Koh CA, Sum A. *Natural Gas Hydrates in Flow Assurance*. Gulf Professional Publishing, Burlington, MA, 2010.
7. Kelland MA, Svartaas TM, Øvsthus J, Namba T. A new class of kinetic hydrate inhibitor. *Ann N Y Acad Sci*. 2000;912(1):281–293.
8. Fu B, Neff S, Mathur A, Bakeev K. Application of low-dosage hydrate inhibitors in deepwater operations. *Old Prod Facil*. 2002;17(3):133–137.
9. Mehta AP, Hebert PB, Cadena ER, Weatherman JP. Fulfilling the promise of low-dosage hydrate inhibitors: journey from academic curiosity to successful field implementation. *Old Prod Facil*. 2003;18(1):73–79.
10. Notz PK, Bumgardner SB, Schaneman BD, Todd JL. Application of kinetic inhibitors to gas hydrate problems. *Old Prod Facil*. 1996;11(4):256–260.
11. Gordienko R, Ohno H, Singh VK, Jia Z, Ripmeester JA, Walker VK. Towards a green hydrate inhibitor: imaging antifreeze proteins on clathrates. *PLoS One*. 2010;5(2):e8953.
12. Zeng H, Wilson LD, Walker VK, Ripmeester JA. The inhibition of tetrahydrofuran clathrate-hydrate formation with antifreeze protein. *Can J Phys*. 2003;81(1–2):17–24.
13. Glenat P, Peytavy J-L, Holland-Jones N, Grainger M. South-Pars phases 2 and 3: the kinetic hydrate inhibitor (KHI) experience applied at field start-up. In: Abu Dhabi International Conference and Exhibition, Abu Dhabi, UAE, 2004.
14. Webb EB, Rensing PJ, Koh CA, Sloan ED, Sum AK, Liberatore MW. High-pressure rheology of hydrate slurries formed from water-in-oil emulsions. *Energy Fuels*. 2012;26(6):3504–3509.
15. Rensing PJ, Liberatore MW, Koh CA, Sloan ED. *Rheological Investigation of Hydrate Slurries*. In *Proceedings of the 6th International Conference on Gas Hydrates (ICGH 2008)*. Vancouver, Canada, 2008.
16. Sinquin A, Palermo T, Peysson Y. Rheological and flow properties of gas hydrate suspensions. *Oil Gas Sci Technol*. 2004;59(1):41–57.
17. Andersson V, Gudmundsson JS. Flow properties of hydrate-in-water slurries. *Ann N Y Acad Sci*. 2000;912(1):322–329.
18. Schüller RB, Tande M, Kvandal H. Rheological hydrate detection and characterization. *Annu Trans Nord Rheol Soc*. 2005;13:83–90.
19. Pinder KL. Time dependent rheology of the tetrahydrofuran-hydrogen sulphide gas hydrate slurry. *Can J Chem Eng*. 1964;42(3):132–138.
20. Daraboina N, Moudrakovski IL, Ripmeester JA, Walker VK, Englezos P. Assessing the performance of commercial and biological gas hydrate inhibitors using nuclear magnetic resonance microscopy and a stirred autoclave. *Fuel*. 2013;105:630–635.
21. Daraboina N, Linga P, Ripmeester J, Walker VK, Englezos P. Natural gas hydrate formation and decomposition in the presence of kinetic inhibitors. 2. Stirred reactor experiments. *Energy Fuels*. 2011;25(10):4384–4391.
22. Daraboina N, Ripmeester J, Walker VK, Englezos P. Natural gas hydrate formation and decomposition in the presence of kinetic inhibitors. 1. High pressure calorimetry. *Energy Fuels*. 2011;25(10):4392–4397.
23. Daraboina N, Ripmeester J, Walker VK, Englezos P. Natural gas hydrate formation and decomposition in the presence of kinetic inhibitors. 3. Structural and compositional changes. *Energy Fuels*. 2011;25(10):4398–4404.
24. Ohno H, Strobel TA, Dec SF, Sloan J, Koh CA. Raman studies of methane–ethane hydrate metastability. *J Phys Chem A*. 2009;113(9):1711–1716.
25. Lachance JW, Dendy Sloan E, Koh CA. Effect of hydrate formation/dissociation on emulsion stability using DSC and visual techniques. *Chem Eng Sci*. 2008;63(15):3942–3947.
26. Yang J, Tohidi B. Characterization of inhibition mechanisms of kinetic hydrate inhibitors using ultrasonic test technique. *Chem Eng Sci*. 2011;66(3):278–283.
27. Zeng H, Walker VK, Ripmeester JA. Approaches to the design of better low-dosage gas hydrate inhibitors. *Angew Chem*. 2007;119(28):5498–5500.
28. Ohno H, Moudrakovski I, Gordienko R, Ripmeester J, Walker VK. Structures of hydrocarbon hydrates during formation with and without inhibitors. *J Phys Chem A*. 2012;116(5):1337–1343.
29. Behzadfar E, Hatzikiriakos SG. Rheology of bitumen: effects of temperature, pressure, CO₂ concentration and shear rate. *Fuel*. 2014;116:578–587.
30. Ballard AL, Sloan ED Jr. The next generation of hydrate prediction: I. Hydrate standard states and incorporation of spectroscopy. *Fluid Phase Equilibria*. 2002;194:371–383.
31. Linga P, Kumar R, Englezos P. Gas hydrate formation from hydrogen/carbon dioxide and nitrogen/carbon dioxide gas mixtures. *Chem Eng Sci*. 2007;62(16):4268–4276.
32. Sharifi H, Ripmeester J, Walker VK, Englezos P. Kinetic inhibition of natural gas hydrates in saline solutions and heptane. *Fuel*. 2014;117:109–117.
33. Zeng H, Moudrakovski IL, Ripmeester JA, Walker VK. Effect of antifreeze protein on nucleation, growth and memory of gas hydrates. *AIChE J*. 2006;52(9):3304–3309.
34. Anderson BJ, Tester JW, Borghi GP, Trout BL. Properties of inhibitors of methane hydrate formation via molecular dynamics simulations. *J Am Chem Soc*. 2005;127(50):17852–17862.
35. Rodahl M, Höök F, Fredriksson C, Keller CA, Krozer A, Brzezinski P, Voinova M, Kasemo B. Simultaneous frequency and dissipation factor QCM measurements of biomolecular adsorption and cell adhesion. *Faraday Discuss*. 1997;107:229–246.
36. Rodahl M, Hook F, Krozer A, Brzezinski P, Kasemo B. Quartz crystal microbalance setup for frequency and Q-factor measurements in gaseous and liquid environments. *Rev Sci Instrum*. 1995;66(7):3924–3930.
37. Zhang JS, Lo C, Couzis A, Somasundaran P, Wu J, Lee JW. Adsorption of kinetic inhibitors on clathrate hydrates. *J Phys Chem C*. 2009;113(40):17418–17420.
38. Peter B, Dagobert K, Iradj R. Influence of liquid hydrocarbons on gas hydrate equilibrium. In: European Petroleum Conference. SPE 25032, Cannes, France, 1992.
39. Jensen L, Thomsen K, von Solms N. Inhibition of structure I and II gas hydrates using synthetic and biological kinetic inhibitors. *Energy Fuels*. 2010;25(1):17–23.
40. Kumar R, Lee JD, Song M, Englezos P. Kinetic inhibitor effects on methane/propane clathrate hydrate-crystal growth at the gas/water and water/n-heptane interfaces. *J Cryst Growth*. 2008;310(6):1154–1166.
41. Lou A, Pethica BA, Somasundaran P. Interfacial and monolayer properties of poly (vinylcaprolactam). *Langmuir*. 2000;16(20):7691–7693.
42. Águila-Hernández J, Trejo A, García-Flores BE. Volumetric and Surface Tension Behavior of Aqueous Solutions of Polyvinylpyrrolidone in the Range (288 to 303) K. *J Chem Eng Data*. 2011;56(5):2371–2378.

Manuscript received July 25, 2013, and revision received Jan. 7, 2014.